coatings

MDPI

*Article*

# Analysis of Mechanical Properties of Fiber Reinforced Concrete Using RCC and PCC

**Jiawei Fan [1,2,3], Yiyu Long [1], Juntao Xu [4], Shumao Qiu [5,*] and Wei Qiao [4]**

[1] China Academy of Railway Sciences, Beijing 100081, China; jiaweif3@163.com (J.F.); along599@163.com (Y.L.)
[2] Railway Engineering Research Institute, China Academy of Railway Sciences Co., Ltd., Beijing 100081, China
[3] National Key Laboratory of High-Speed Railway Track System, China Academy of Railway Sciences Co., Ltd., Beijing 100081, China
[4] School of Engineering and Technology, China University of Geosciences (Beijing), Beijing 100083, China; xjt_329@163.com (J.X.); 3102230001@email.cugb.edu.cn (W.Q.)
[5] Research Institute of Highway, Ministry of Transport, Beijing 100088, China
* Correspondence: sm.qiu@rioh.cn

**Abstract:** The addition of macro fibers to concrete pavements has been used to improve the cracking of concrete pavement, reduce slab thickness and contribute to increasing the joint spacing. A laboratory test was carried out in the study to analyze the impact of fiber reinforced concrete (FRC) on plain cement concrete (PCC) and roller compacted concrete (RCC), determining the flexural strength by performing ASTM-1609 tests and compressive strength by ASTM C-39 tests. Two synthetic fiber types selected with different geometries and different dosages (0.25% and 0.5% by volume) were tested for both RCC and PCC. To examine the effect of fiber contents and property, statistical testing was done using strength-test data. The test result showed that flexural strength was not affected by fibers. As fiber content increased, both residual strength ($F_{600}$ and $F_{150}$) and specimen toughness ($T_{150}$) increased for each fiber type. To the contrary, the compressive strength of specimens with higher fiber contents was lower in every case. Fiber properties including length and shape affected the residual strength of RCC more, than PCC. It is notable that the residual strength of RCC and PCC with the same fiber condition is very similar, even though the mix design and compressive and flexural strengths are different. In this paper, the strength-test data results are discussed, and the factors affecting the test results and the limitations of the testing methods are suggested.

**Keywords:** fiber reinforced concrete; flexural strength; compressive strength; RCC; PCC

check for updates

**Citation:** Fan, J.; Long, Y.; Xu, J.; Qiu, S.; Qiao, W. Analysis of Mechanical Properties of Fiber Reinforced Concrete Using RCC and PCC. *Coatings* **2024**, *14*, 972. https://doi.org/10.3390/coatings14080972

Academic Editor: Paolo Castaldo

Received: 13 June 2024
Revised: 25 July 2024
Accepted: 31 July 2024
Published: 2 August 2024

**Copyright:** © 2024 by the authors. Licensee MDPI, Basel, Switzerland. This article is an open access article distributed under the terms and conditions of the Creative Commons Attribution (CC BY) license (https://creativecommons.org/licenses/by/4.0/).

## 1. Introduction

Over the years, roller compacted concrete (RCC) has been used for pavements in storage areas, municipal and industrial roads [1] with the availability of design procedures for industrial pavements [2] and roadways [3]. Roller compacted concrete has become a popular alternative pavement type because of the expedient construction benefits (earlier opening to traffic), reduced material and construction costs, increased sustainability rating, and structural capacity [4]. RCC has reduced the amount of cement due to the increase in the percentage of aggregate content, continuous gradation, and compaction energy [5]. In the case of fiber reinforcement in RCC with the addition of fibers, the flexural toughness and residual strength increases. Properly designed macro fibers in RCC lead to thickness reduction and crack width reduction which gives enhanced aggregate interlock joints and a reduction in the rate of crack deterioration [6,7]. Plain cement concrete (PCC) has low flexural strength and crack-holding capacity. The addition of fibers tremendously increases its structural characteristics and allows a reduction in concrete pavement thickness [8,9]. Therefore, the addition of fibers to concrete has become a common approach to improve its crack-holding capacity. A series of research projects has been carried out to investigate

the physical and mechanical properties of RCC or PCC with the addition of different types of fibers.

Zhao et al. (2024) [10] investigated the influence of recycled-tire steel fiber length on the mechanical properties of steel fiber-reinforced concrete, claiming that fibers with a length of 21 mm are the optimum for the mixture design. Otieno and Mushunje (2021) [11] investigated the influence of replacement of fine mineral aggregates with crumb tire rubber of different particle sizes on the creep and shrinkage of PCC, claiming that it has similar creep and shrinkage deformation characteristics to that of mineral aggregate concrete. Isa et al. (2020) [12] contended that adding the hybrids of recycled-tire steel cords and recycled-tire steel fibers can achieve the desired flexural strength of the mixture. Akhtar et al. (2022) [13] concluded that 0.25%–0.5% recycled-tire steel fiber can enhance the ductility and imperviousness of concrete. Alwesabi et al. (2021) and Neves et al. (2024) [14,15] proved that adding recycled-waste tires to concrete is beneficial to its fracture characteristics.

Besides adding tire fiber, basalt, PVA, waste glass, and sisal fibers were also utilized in concrete mixtures. Yang et al. (2023) [16] performed three-point bending testing and concluded that AP interleaving is confirmed as an effective method in improving the interlayer structure and flexural performance of basalt fiber-reinforced polymer composites. Similarly, Meyyappan and Carmichael (2021) [17] confirmed that basalt fiber-reinforced concrete can enhance the strength properties of concrete. Alomayri (2021) [18] investigated the mechanical properties of basalt fiber-reinforced fly ash-based geopolymer pastes with various contents of additions, concluding that 3% nano $CaCO_3$ in basalt fiber-reinforced geopolymer paste presented the highest values of compressive strength. Yildizel et al. (2022) [19] proposed the optimal mixture design for basalt fiber-reinforced RCC. Wang et al. (2023) [20] investigated the physical and mechanical properties of basalt and sisal fiber-mixed concrete, concluding that the optimal hybrid fibers volume fraction was calibrated at 0.3%. Mitani et al. (2022), Yao et al. (2024), Min et al. (2024), Rao et al. (2022) and Wan et al. (2020) [21–25] confirmed that adding PVA fibers can contribute to the enhancement of the mechanical properties of the mixture. Gencel et al. (2022), Ibrahim (2021), Zeybek (2022), Ali et al. (2021) and Gholampour et al. (2022) [26–30] reported that the addition of waste glass improves the physico-mechanical and durability properties of the concrete. Jamshaid et al. (2022) [31] concluded that the addition of sisal improves the mechanical properties of the concrete when the content of additions is up to 2%. Sreekumaran et al. (2024) [32] confirmed that sisal hybrid fiber-reinforced concrete has a similar mechanical property compared with the usage of steel fibers in concrete when its addition is within 25%. Kerche et al. (2022) [33] investigated the physical and mechanical properties of hybrids of PVA, waste glass, and sisal fibers, reporting that adding glass fiber can achieve a higher flexural stiffness and modulus.

To thoroughly investigate the flexural strength and compressive strength of RCC and PCC with reinforcement of synthetic macro-fibers, a series of tests was conducted in this study. ASTM C1399 and C1609 [34–38] are the most common tests for evaluating FRC materials for bridge deck, deck overlays and pavement overlays (ACI Committee 544 2018). ASTM-1609 provides several performance measures of the combined interaction between concrete and macro fibers. The residual strength ($f_{150}$) and the equivalent flexural strength ratio (RT,150) are calculated from the monotonic-load deflection curve of a flexural beam specimen till 1/8 in deflection. There are shortcomings to the test as well. Banthia and Islam [39] discussed the limitations of the ASTM-1609 test and raised numerous concerns specifically concerning the loading rate [40].

Adding fibers to RCC and PCC and conducting comparative experiments helps to comprehensively evaluate the performance of fibers in these two types of concrete, providing a basis for engineering applications and gaining a deeper understanding of the material characteristics of the two types of concrete. This is of great significance for the design and construction of concrete structures. Since there are limited studies carried out previously on studying the effects of macro fibers (specifically synthetic fibers) in RCC, the objective of the paper is to compare the mechanical properties obtained for RCC and PCC mixed with fibers and discuss the influence of different types and volumes of fibers in the flexural

strength of concrete. The study will also address the limitations of the ASTM-1609 test and address solutions for the same.

## 2. Testing Materials

### *2.1. Mix Design Properties*

The performance of RCC and PCC highly depends on the mixture design. An appropriate water content and water-to-cement ratio intrinsically influences the workability and strength of the concrete. The strength of concrete has an inverse relationship with the water-to-cement ratio. However, slightly increasing the water content is beneficial to the workability. Therefore, balancing between them is critical for concrete mixture design. In addition, aggregate gradation has a significant influence on the performance of concrete. In this study, oven-dried coarse dolomite, intermediate dolomite, and natural sand are chosen based on the 0.45 power maximum density curve, which showed a satisfactory result in the previous study [6]. In terms of types of macrofibres, two different synthetic fibers with different surface textures are used in this study. As for the fibers' dosage, 0.2% to 0.5% by volume is a typical range of the fiber content. Additionally, Min et al. (2024) [23] claimed that a significant improvement in the fatigue life of the concrete was observed when adding PVA fiber at a volume fraction of 0.2%. Similarly, Akhtar et al. (2022) [13] concluded that 0.25%–0.5% by volume fibers can enhance the ductility and imperviousness of concrete. Therefore, the amounts of 0.25% and 0.5% by volume fibers are used for each type of synthetic fiber. The mixture proportions of each component for RCC are shown in Table 1. The mixture proportions of each component for PCC are shown in Table 2.

**Table 1.** Mixture proportions of RCC (kg/m$^3$).

| Batch (Kg) | 0.25% Volume Fiber | 0.5% Volume Fiber |
|---|---|---|
| Coarse Dolomite (Oven dry) | 534.89 | 534.29 |
| Intermediate Dolomite (Oven dry) | 962.78 | 961.74 |
| Natural Sand (Oven dry) | 641.85 | 641.16 |
| Cement | 288.67 | 288.67 |
| Water | 157.27 | 157.27 |
| Fibers | 2.33 | 4.67 |
| Total | 2587.81 | 2587.81 |

**Table 2.** Mixture proportions of PCC (kg/m$^3$).

| Batch (lb) | 0.25% Volume Fiber | 0.5% Volume Fiber |
|---|---|---|
| Coarse Dolomite (Oven dry) | 1048.53 | 1044.71 |
| Natural Sand (Oven dry) | 656.46 | 657.36 |
| Cement | 337.99 | 338.46 |
| Water | 192.28 | 192.55 |
| Fibers | 2.10 | 4.29 |
| Total | 2237.37 | 2237.37 |

### *2.2. Information about Fibers*

Two different synthetic fibers are used in this study. The detailed information is shown in Table 3.

**Table 3.** Information about fibers.

| Characteristic | A | B |
|---|---|---|
| Fiber Name | BarChip MQ58 | Fibermesh 4 Roads |
| Material | Bi-Component Polymer | blend of two homopolymer polypropylene fibers:<br>- Macro-monofilament fibers<br>- Micro synthetic grade fibers |
| Length | 58 mm | 65 mm |
| Tensile Strength | 640 Mpa | 613 Mpa (Macro-monofilament fibers) |
| Texture | Continuous Embossing | Continuous Embossing (Macro-monofilament fibers)<br>Flat (Micro synthetic fibers) |

## 3. Concrete Beam and Cylinder Fabrication

### *3.1. Mixing Procedure*

The mixing procedure was conducted based on ASTM C192 (2018), described as follows. Weight the materials including oven dried coarse dolomite, intermediate dolomite, natural sand, cement, water, and fibers separately. Mix the coarse dolomite, intermediate dolomite, natural sand, and half amount of the water in the mixer for one minute. Add cement and the other half amount of water into the mixture mixing for three minutes. Add fibers evenly into the mixture mixing for two minutes. Check whether fibers are balling or clumping, and evenly distribute fibers in the mixture by hand, and mix for one more minute (Figure 1).




**Figure 1.** Mixer for Mixture.

### *3.2. Casting Procedure*

Based on the ASTM D1557 and ASTM C1435, electric vibrating hammer is used to mold RCC beams and cylinders. Three replicate beams and three cylinders are fabricated for each fiber type and fiber dosage for RCC as well as PCC. The beam is 18 in. in length and has 6 in. by 6 in. cross section. The cylinder is 4 in. in diameter and 8 in. in height. The beams are subjected to third-point loading testing for flexural performance of fiber-reinforced concrete at 15 to 18 days, and the cylinders are subjected to compressive strength testing at 28 days (Figure 2).



**Figure 2.** Beams and Cylinders of PCC and RCC.

## 4. Testing Procedure

### *4.1. ASTM 1609 Third-Point Loading Testing for Flexural Performance of FRC*

ASTM C1609-12 is used as the test method to analyze concrete beam performance with reinforced fibers. The testing is based on a simple supported beam under third-point loading (Figure 3). Instead of regular load-controlled testing, it is controlled by the mid-span vertical deflection. The testing terminates when the mid-span vertical deflection reaches $L/150$. Typically, when $L$ is equal to 18 in., $L/150$ is equal to 0.12 in.

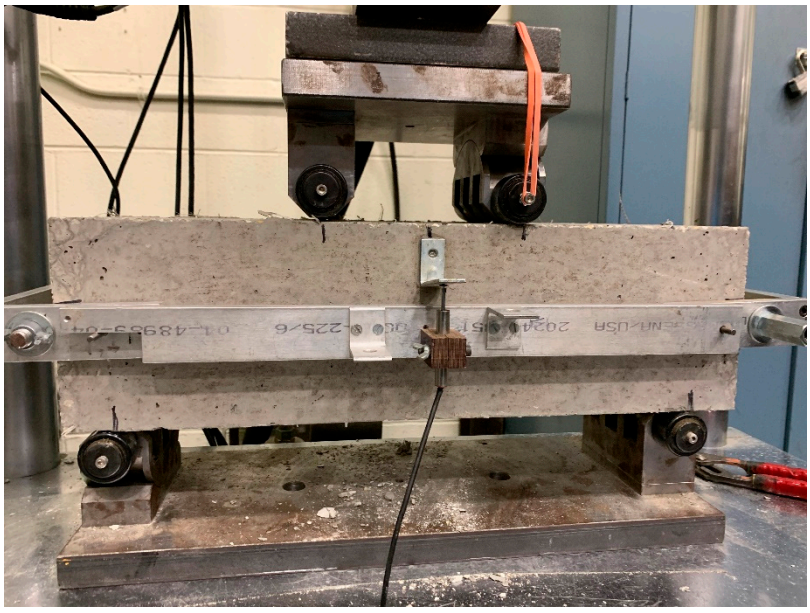


**Figure 3.** ASTM C1609-12 testing apparatus.

As for the dimension of the beam specimen in this study, 6 in. square cross section and 18 in span is adopted.

Several parameters are of great interest in this testing method, including peak strength, residual strength at net deflection of $L/600$, residual strength at net deflection of $L/150$, specimen toughness, and equivalent flexural strength ratio. The first-peak strength, usually the peak strength, is the indication of beginning of cracking. The residual strength indicates the capability of holding the cracks by fibers after cracking. The specimen toughness indicates the capacity of energy absorption of the specimen.

The following formulas explain the way to calculate such parameters. Figures of the specimens after testing are attached in Appendix D.

$$f_1 = \frac{P_1 L}{bd^2} \tag{1}$$

$$f_{150}^D = \frac{P_{150}^D L}{bd^2}, \tag{2}$$

$$f_{600}^D = \frac{P_{600}^D L}{bd^2}, \tag{3}$$

$$R_{T,150}^D = \frac{150 T_{150}^D}{f_1 bd^2} \times 100(\%), \tag{4}$$

where

$P_1$ is the peak load as well as the first-peak load;
$L$ is the span length of beams;
$b$ is the width of the cross section, and $d$ is the depth of the cross section;
$f_1$ is the peak strength as well as the first-peak strength;
$P_{150}^D$ is the load obtained from load-deflection curve when the mid-span vertical deflection reaches $L/150$;
$f_{150}^D$ is the residual strength of FRC at the net deflection of $L/150$;
$P_{600}^D$ is the load obtained from load-deflection curve when the mid-span vertical deflection reaches $L/600$;
$f_{600}^D$ is the residual strength of FRC at the net deflection of $L/600$;
$T_{150}^D$ is the area under the load-deflection curve from 0 to $L/150$;
$R_{T,150}^D$ is the equivalent flexural strength ratio.

### 4.2. ASTM C39 Compressive Strength Testing

ASTM C39 is used to analyze the concrete cylinder compressive strength. By applying a compressive axial loading to the cylinder specimen at a loading rate until the cylinder is failed, calculate the strength of the concrete cylinder by loading at the failure divided by the cross section of the cylinder. The loading rate should be in the range from 12 MPa/min to 18 MPa/min. The cylinder specimen alignment should be verified since unbounded caps are used in this study. Figures of the specimens after testing are attached in Appendix E.

$$f_{cm} = \frac{4P_{max}}{\pi D^2} \tag{5}$$

where

$P_{max}$ is the maximum load when cylinder fails;
$D$ is the average measured diameter;
$f_{cm}$ is the compressive strength.

## 5. Testing Results

### 5.1. Compressive Strength

Figure 4 and Table 4 show the compressive strength properties. As expected, the compressive strength of the RCC specimens is higher than that of the PCC specimens. For every PCC and RCC specimen, specimens which have 0.5% volume fiber have a smaller compressive strength than specimens which have 0.25%.

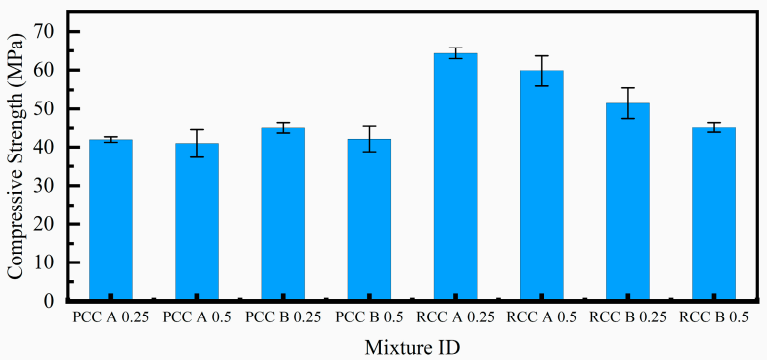



**Figure 4.** Compressive strength testing results.

**Table 4.** Compressive strength testing results.

| | Compressive Strength [MPa] | |
|---|---|---|
| **Mixture ID** | **Average** | **COV (%)** |
| PCC A 0.25 | 42.001 | 0.764 |
| PCC A 0.5 | 40.997 | 3.612 |
| PCC B 0.25 | 45.044 | 1.304 |
| PCC B 0.5 | 42.150 | 3.357 |
| RCC A 0.25 | 64.357 | 1.415 |
| RCC A 0.5 | 59.858 | 3.827 |
| RCC B 0.25 | 51.476 | 4.063 |
| RCC B 0.5 | 45.158 | 1.219 |

### *5.2. Flexural Strength*

#### 5.2.1. Strength Properties

Figure 5 and Table 5 show the flexural performance testing results. For all strength parameters, the coefficient of variation (COV) is calculated to account for the data point dispersion. Peak flexural strengths (MOR) are calculated for all cases including PCC and RCC, but the residual strength ($F_{600}$ and $F_{150}$), specimen toughness ($T_{150}$) and equivalent flexural strength ratio (RT,150) of some specimens could not be calculated because of the testing failure after peak strength (Appendix C). The detailed reason for the testing failure will be discussed in the following Discussion Section. The load-deflection curves of RCC and PCC are plotted and compared in Figure 6. RCC samples were subjected to reloading as this failed at the initial attempt. Detailed discussion of the initial failure is found in Section 6.7.

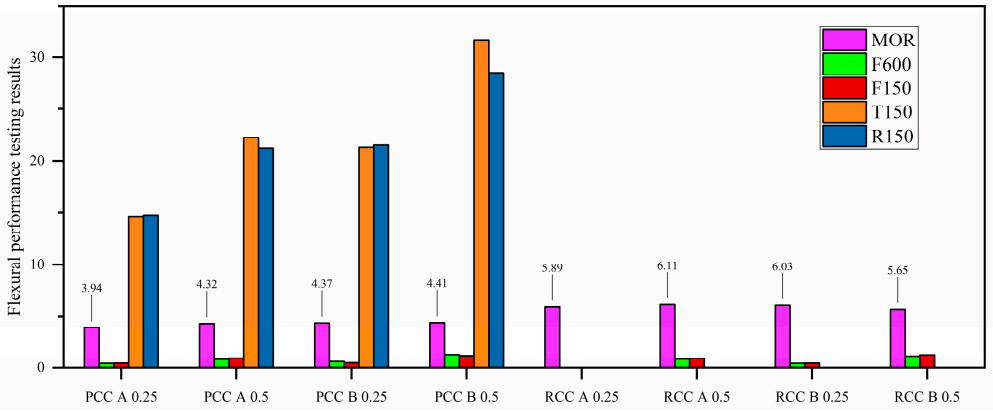



**Figure 5.** Flexural performance testing results.

**Table 5.** Flexural performance testing results.

| | MOR [MPa] | | $F_{600}$ [MPa] | | $F_{150}$ [MPa] | | $T_{150}$ [Nm] | | $R_{150}$ [%] | |
|---|---|---|---|---|---|---|---|---|---|---|
| **Mixture ID** | **Average** | **COV (%)** | **Average** | **COV (%)** | **Average** | **COV (%)** | **Average** | **COV (%)** | **Average** | **COV (%)** |
| PCC A 0.25 | 3.942 | 4.80 | 0.430 | 34.85 | 0.446 | 31.55 | 14.627 | 17.51 | 14.754 | 12.84 |
| PCC A 0.5 | 4.321 | 6.78 | 0.816 | 26.90 | 0.934 | 39.07 | 22.297 | 38.87 | 21.230 | 31.24 |
| PCC B 0.25 | 4.370 | 6.08 | 0.601 | 54.46 | 0.484 | 67.88 | 21.315 | - | 21.535 | - |
| PCC B 0.5 | 4.408 | 4.04 | 1.301 | 1.81 | 1.170 | 7.02 | 31.685 | 1.65 | 28.525 | 3.90 |
| RCC A 0.25 | 5.893 | 7.91 | - | - | - | - | - | - | - | - |
| RCC A 0.5 | 6.111 | 5.50 | 0.835 | - | 0.921 | 13.54 | - | - | - | - |
| RCC B 0.25 | 6.031 | 4.33 | 0.433 | - | 0.441 | 32.46 | - | - | - | - |
| RCC B 0.5 | 5.654 | 14.27 | 1.137 | 25.62 | 1.251 | 15.21 | - | - | - | - |

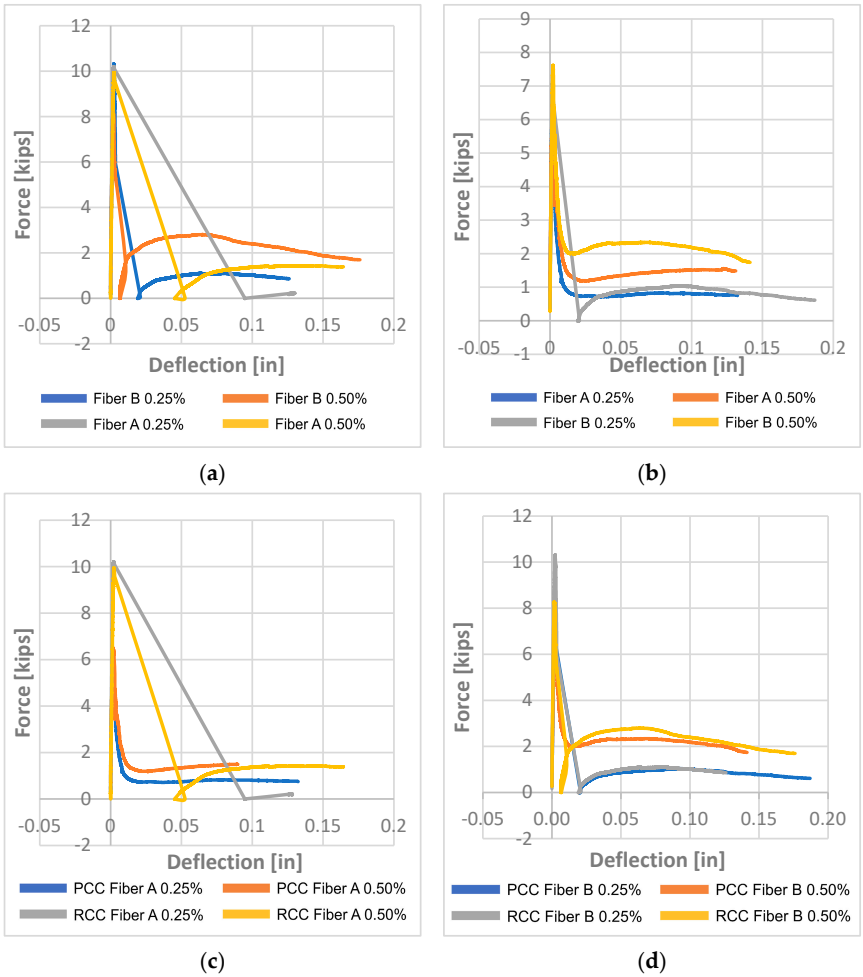



**Figure 6.** Force vs. Deflection graph of RCC and PCC. (**a**) Force vs. Deflection chart for RCC; (**b**) Force vs. Deflection chart for PCC; (**c**) Force vs. Deflection chart for RCC and PCC; (**d**) Force vs. Deflection chart for RCC and PCC.

5.2.2. Statistical Analysis

Tables 6–8 shows the statistical analysis results for the flexural strength (MOR) and residual strength ($F_{600}$ and $F_{150}$), respectively. For MOR values, a *t*-test with a 95% confidence interval was conducted to compare the effect of fiber contents and fiber properties. Since our hypothesis based on the previous research is that the flexural strength is not affected by fibers [6,9], a two-tailed *t*-test was adopted. For residual strengths, it is assumed that the fiber content and fiber properties affect values, thus a one-tailed *t*-test was conducted. Based on the reference value 0.05, statistical significance was shown in the tables.

**Table 6.** Statistical Analyses of Flexural strength characteristics.

| Test No. | Mixture ID | MOR [MPa] | std.dev | *t*-Test | Two Sided *p*-Value | Statistically Significant? |
|---|---|---|---|---|---|---|
| 1 | PCC A 0.25<br>PCC A 0.5 | 3.942<br>4.321 | 0.189<br>0.293 | −1.88224 | 0.156349 | No |
| 2 | PCC B 0.25<br>PCC B 0.5 | 4.370<br>4.408 | 0.266<br>0.178 | −0.20758 | 0.848849 | No |
| 3 | PCC A 0.5<br>PCC B 0.5 | 4.321<br>4.408 | 0.293<br>0.178 | −0.44173 | 0.688585 | No |
| 4 | PCC A 0.25<br>PCC B 0.25 | 3.942<br>4.370 | 0.189<br>0.266 | −2.27181 | 0.085556 | No |
| 5 | RCC A 0.25<br>RCC A 0.5 | 5.893<br>6.111 | 0.466<br>0.336 | −0.65492 | 0.548271 | No |
| 6 | RCC B 0.25<br>RCC B 0.5 | 6.031<br>5.654 | 0.261<br>0.807 | 0.769449 | 0.522077 | No |
| 7 | RCC A 0.25<br>RCC B 0.25 | 5.893<br>6.031 | 0.466<br>0.261 | −0.4465 | 0.685498 | No |
| 8 | RCC A 0.5<br>RCC B 0.5 | 6.111<br>5.654 | 0.336<br>0.807 | 0.904236 | 0.432524 | No |

**Table 7.** Statistical Analyses of Residual strength characteristics, $F_{600}$.

| Mixture ID | $F_{600}$ [MPa] | std.dev | *t*-Test | One Sided *p*-Value | Statistically Significant? |
|---|---|---|---|---|---|
| PCC A 0.25<br>PCC A 0.5 | 0.430<br>0.816 | 0.150<br>0.219 | −2.51038 | 0.033015 | Yes |
| PCC B 0.25<br>PCC B 0.5 | 0.601<br>1.301 | 0.327<br>0.024 | −3.02126 | 0.101744 | No |
| PCC A 0.5<br>PCC B 0.5 | 0.816<br>1.301 | 0.219<br>0.024 | −3.80898 | 0.031265 | Yes |
| PCC A 0.25 | 0.430 | 0.150 | | | |
| PCC B 0.25 | 0.601 | 0.327 | −0.68931 | 0.307895 | No |

**Table 8.** Statistical Analyses of Flexural strength characteristics, $F_{150}$.

| Mixture ID | $F_{150}$ | std.dev | *t*-Test | One Sided *p*-Value | Statistically Significant? |
|---|---|---|---|---|---|
| PCC A 0.25 | 0.446 | 0.141 | | | |
| PCC A 0.5 | 0.934 | 0.365 | −2.16242 | 0.059651631 | No |
| PCC B 0.25 | 0.484 | 0.328 | | | |
| PCC B 0.5 | 1.170 | 0.082 | −3.51385 | 0.036157444 | Yes |
| PCC A 0.5 | 0.934 | 0.365 | | | |
| PCC B 0.5 | 1.170 | 0.082 | −1.09404 | 0.194060157 | No |
| PCC A 0.25 | 0.446 | 0.141 | | | |
| PCC B 0.25 | 0.484 | 0.328 | −0.18385 | 0.432928007 | No |
| RCC B 0.25 | 0.441 | 0.143 | | | |
| RCC B 0.5 | 1.251 | 0.190 | −5.89291 | 0.00207353 | Yes |
| RCC A 0.5 | 0.921 | 0.125 | | | |
| RCC B 0.5 | 1.251 | 0.190 | −2.50748 | 0.043565324 | Yes |

## 6. Discussion

### *6.1. Effect of Fiber Contents*

To figure out the effect of fiber contents for flexural strength and residual strength, a *t*-test for each specimen with different fiber contents was conducted. Table 6 shows the *t*-test results for flexural strength of the specimens. Test numbers 1 and 2 are the testing results for PCC with different fiber contents, and test numbers 5 and 6 are the test results for RCC with different fiber contents. As expected, all case results are not statistically significant, which means that the flexural strength is not affected by fiber content. This is because the role of fibers is holding the crack after peak stress, so fibers have no influence on flexural strength before cracking.

Tables 7 and 8 shows the statistical test results for residual strengths $F_{600}$ and $F_{150}$. Due to the flexural testing failure, all the $F_{600}$ values and some $F_{150}$ values of RCC could not be calculated. For all cases including PCC and RCC, the residual strength of specimens with 0.5% fibers is greater than that of specimens with 0.25% fibers, from 89% to 184%. This is also clearly shown in Figure 4.

From Table 7, the *t*-test result for PCC with fiber A shows that more fiber increases the $F_{600}$ residual strength statistically. Although the *t*-test result from PCC with fiber B is not statistically different with fiber content, the *p*-value is almost at threshold (0.05). In the case of $F_{150}$ residual strength, both PCC and RCC with fiber B are statistically affected by fiber content. Again, the $F_{150}$ residual strength of PCC with fiber A is not statistically different with fiber content, but the *p*-value is almost at threshold (0.05). Considering that the threshold *p*-value is frequently used up to 0.1, it is clearly shown that the higher fiber content increases the residual strength of both RCC and PCC.

Although the specimen toughness and equivalent flexural strength ratio were only calculated for PCC specimens, it also shows the effect of fibers. In Table 5, for both fibers, specimen toughness was increased from 32% to 52% by using more fiber content. According to ASTM 1609, specimen toughness is a measure of the energy absorption capacity of the test specimen.

As the fiber contents increased, the values of both residual strength ($F_{600}$ and $F_{150}$) and specimen toughness ($T_{150}$) increased for each fiber type. This result is in accordance with previous research on FRC [6,9].

In Table 4, the compressive strength of specimens with higher fiber content is lower in every case. Increased fiber content may prevent aggregate contact and create a weaker zone in the specimen.

### *6.2. Effect of Fiber Properties*

To examine the effect of different fiber properties, the test results of PCC and RCC with the same fiber content and different fiber materials were compared and statistically tested. Table 6 shows that the flexural strength of specimens with different fibers is not statistically different. As discussed in previous paragraphs, this is because fibers have no influence on flexural peak strength.

Table 8 shows the residual strength ($F_{150}$) of each specimen and the statistical testing results. For PCC specimens, although the $F_{150}$ values of specimens with Fiber B were greater than those of specimens with Fiber A, a comparison between specimens with different fibers shows no statistical difference. That means the fiber material difference did not affect the residual strength of the PCC beams. However, the residual strength of RCC specimens with fiber B is 36% greater than the residual strength of RCC specimens with fiber A, and statistical testing results also shows the significant difference. That means that fiber B is better than fiber A, in terms of the residual strength of RCC.

Unlike PCC specimens, the RCC mixing procedure and gradation makes fiber bent and tortuous. This may result in the fiber length at the failure plane not being enough to resist the tensional stress. Considering Fiber B is 12% longer than fiber A, a longer fiber length could be a reason for the greater residual strength. Another possible reason is the texture of fibers. Half of the fiber B specimens were very flexible and flat, whereas all the fiber A specimens were continuously embossing and stiffer. The flexible and flat component of fiber B may allow the fiber to have a tortuous and bendy shape along the aggregates in RCC.

From Table 4, the compressive strength of the RCC specimens with fiber B is significantly lower than that of the RCC specimens with fiber A. Having longer and flexible fibers brings better residual strength but decreases compressive strength because it prevents particle contacts in RCC.

### *6.3. Residual Strength of RCC and PCC*

Table 9 shows the comparison of residual strength between RCC and PCC specimens. Even though the RCC and PCC specimens have a different mixing design, and compressive and flexural strength, the residual strength of specimens with the same fibers and same fiber contents shows an almost identical trend of residual strength. This result could be evidence that the residual strength is governed by the fiber property and fiber contents, not the concrete mixing properties.

**Table 9.** Residual strength of RCC and PCC.

| Fiber, Content (%) | $F_{600}$ [MPa] | | | $F_{150}$ [MPa] | | |
|---|---|---|---|---|---|---|
| | RCC | PCC | Difference (%) | RCC | PCC | Difference (%) |
| A, 0.25 | - | 0.430 | | - | 0.446 | |
| A, 0.5 | 0.835 | 0.816 | 2.3 | 0.921 | 0.934 | 1.4 |
| B, 0.25 | 0.433 | 0.601 | 11.9 | 0.441 | 0.484 | 8.9 |
| B, 0.5 | 1.137 | 1.301 | 12.6 | 1.251 | 1.170 | 6.5 |

### *6.4. Comparison of Testing Results with Other Studies in the Literature*

The comparison of mechanical properties of FRC between this study and others in the literature is displayed in Table 10. The comparison results indicate that the fibers A and B used in this study have a higher performance at the same dosage compared to fibers added in other studies.

**Table 10.** FRC mechanical properties comparison between this study and others in the literature.

| | Flexural Strength (MPa) | Compressive Strength (MPa) |
|---|---|---|
| PCC PVA 1.50, literature [41] | 4.34 | 46.86 |
| PCC PVA 0.20, literature [23] | 4.50 | - |
| PCC Basalt 0.50, literature [17] | 4.88 | 34.08 |
| PCC Glass 10.0, literature [28] | 5.93 | 18.10 |
| RCC without fibers, literature [19] | 4.35 | 35.15 |
| RCC without fibers, literature [6] | 4.65 | 46.70 |
| PCC A 0.25, this study | 3.942 | 42.001 |
| PCC A 0.50, this study | 4.321 | 40.997 |
| PCC B 0.25, this study | 4.370 | 45.044 |
| PCC B 0.50, this study | 4.408 | 42.150 |
| RCC A 0.25, this study | 5.893 | 64.357 |
| RCC A 0.50, this study | 6.111 | 59.858 |
| RCC B 0.25, this study | 6.031 | 51.476 |
| RCC B 0.50, this study | 5.654 | 45.158 |

### *6.5. Effects Analysis of Fiber-Reinforced Concrete*

#### 6.5.1. Cost Analysis

The economy of FRC is mainly reflected in the following aspects. Firstly, although the addition of fibers increases the cost per unit volume of concrete, from the perspective of total lifecycle cost, FRC often has a lower total cost than ordinary concrete due to its reduced frequency of maintenance and replacement. Furthermore, FRC has excellent crack resistance, which helps to reduce leakage problems caused by cracks and lower additional costs due to water damage.

#### 6.5.2. Environmental Impact Assessment

FRC has significant environmental benefits in the production process. FRC reduces cement consumption and correspondingly lowers carbon emissions during production by adding different types of fibers, which helps to slow down the trend of global climate change. Secondly, FRC has higher crack resistance, impermeability, and durability, which means that FRC is less prone to cracking and leakage during use, thereby reducing the frequency of repairs and replacements and lowering the maintenance costs. Meanwhile, due to the better durability and longer service life, it further reduces the generation of construction waste and lowers the pressure on the environment. In addition, FRC also has good renewability. With the continuous development of the construction industry, the problem of construction waste is becoming increasingly serious. The fiber materials in FRC can be recycled and reused to reduce the amount of construction waste.

#### 6.5.3. Concrete Workability

After adding fibers to concrete, the slump of concrete tends to decrease, indicating that the addition of fibers reduces the fluidity of concrete. The mechanism of the influence of fibers on the workability of freshly mixed concrete is that the fibers are randomly distributed in the mixture, providing support for the various components of the mixture, causing an increase in internal friction and a decrease in the fluidity and workability of the mixture. Meanwhile, the addition of fibers increases the surface area and occupies a large amount of water, thereby reducing the slump of concrete.

### *6.6. Factors' Effects on Testing Results*

#### 6.6.1. Curing Time

Curing time is a key determinant to the strength of concrete specimens for both PCC and RCC. The strength of concrete specimens would have been increasing during the 28 days after casting. However, not all of the specimens were well cured by the moisture due to the damage of the moisture curing room, which had a significant influence on the strength of the specimens. To be specific, six RCC beams mixed using fiber type A were cured in the moisture room for 2 days and were dry cured for 18 days. Six PCC beams mixed using fiber type A were dry cured for 17 days. Six RCC beams mixed using fiber type B were dry cured for 17 days. Six PCC beams mixed using fiber type B were dry cured for 15 days. All the twenty-four cylinders were dry cured for 28 days.

#### 6.6.2. Eccentricity

Certain samples while testing using the ASTM-1609 test had an eccentricity in the third-point loading. According to ASTM 1609 specifications, third-point loading should be applied without any eccentricity to samples. The results of the samples that had eccentricity caused the low peak as well as residual strength. Samples for RCC 0.25% fiber A sample 3, 0.50% fiber A sample 2, RCC 0.50% fiber B samples 1 and 3, 0.25% fiber B sample 3, and for PCC 0.5% fiber A sample 1 and 0.5% fiber B sample 2 had eccentricities while loading. Some lower values from the samples that had eccentricity were excluded from data analysis. Load-deflection curves for the samples are attached in Appendix A.

#### 6.6.3. Compaction

As for the compaction process, the RCC beam and cylinder specimens were cast according to ASTM D1557-12 and ASTM 1435 standard. A vibrating hammer was used to cast the specimens. However, the hammer rod was broken when molding the RCC mixture with fiber type A. Since the casting process could not be stopped otherwise new mixtures should be made again and there were only two beams and three cylinders left, we chose to put the head of the vibrating hammer on the mixture and put the rod in contact with it to continue compaction. We expected that the strength of these beams and cylinders might be lower than others because of the nonuniform distributed load of compaction. However, the results show that the strength of these beams and cylinders is at the same level as the others.

### *6.7. Limitation of Testing Methods*

ASTM 1609 is one of the most common tests to analyze the performance of FRC. However, ASTM 1609 still has several limitations that would make it difficult to obtain a stable load-deflection curve.

The first factor is related to 'closed-loop control' machines. According to Banthia and Islam [39], there is a huge probability that a closed-loop machine cannot control stability. Many factors rather than the testing material itself would influence controlling stability. In this study, the stiffness of the loading frame is a key determinant of obtaining a stable load-deflection curve because the loading frame itself is not sufficiently stiff. The machine would wrongly recognize that the testing beam has been failed, especially for RCC which has a higher flexural strength. Since the sudden stop of the testing machine, the load-deflection curve could not be obtained.

The second factor is the loading rate in the ASTM 1609 specifications. According to Banthia and Islam [39], the specified loading rate in ASTM 1609 is too high especially for low-dosage fiber-content concrete. When they conducted ASTM 1609 testing for 1.0 kg/m$^3$ fiber content FRC following a specified loading rate, the stable load-deflection curve could not be obtained. However, if they reduced the loading rate to some extent, a stable load-deflection curve could be acquired. Therefore, they decided to reduce the loading rate to 0.001 to 0.015 mm/min when the net deflection was below $L/900$ and increase the loading rate to 0.02 to 0.15 mm/min after the net deflection reached $L/900$.

## 7. Conclusions

(1) The flexural strength of the concrete is not affected by the type and volume of fibers.
(2) The volume and type of fibers significantly affected the residual strength of both RCC and PCC. Both RCC and PCC showed a marked increase in the residual strength with the increase in the fiber content.
(3) The performance of fiber B was found to be much better than fiber A in terms of the residual strength for RCC. The longer fiber length and flexible components of fiber B could be a reason for this difference in residual strength. Fiber B is more suitable for use in RCC.
(4) There is a decrease in the compressive strength of FRC for each RCC and PCC.
(5) The residual strength of RCC and PCC with the same fiber condition is very similar, although the mix design and compressive and flexural strength are different. This could be because the residual strength is governed by fiber property and fiber content, not the concrete mixing properties.

**Author Contributions:** Conceptualization, J.F.; methodology, S.Q.; formal analysis, J.F.; resources, Y.L.; data curation, W.Q.; writing—original draft preparation, J.F.; writing—review and editing, J.X.; supervision, S.Q.; funding acquisition, J.F. All authors have read and agreed to the published version of the manuscript.

**Funding:** This research was funded by Qinghai Province Key Research and Development and Transformation Plan, grant number 2022-SF-158. This research was also funded by China Academy of Railway Sciences Co., Ltd. fund program, grant number 2022YJ333. The funder was not involved in the study design, collection, analysis, interpretation of data, the writing of this article or the decision to submit it for publication.

**Institutional Review Board Statement:** Not applicable.

**Informed Consent Statement:** Not applicable.

**Data Availability Statement:** Data is contained within the article.

**Acknowledgments:** Our team would like to give special thanks to Omar Jadallah and Jordan Ouellet for assisting us in the sample preparation and testing as well as guiding us on the project work. We would also like to thank Jamar Brown for his assistance in sample preparation. Finally, we are very grateful to Jeffery Roesler, for giving us the opportunity and assistance for successful completion of the article.

**Conflicts of Interest:** Author J.F. was employed by the company Railway Engineering Research Institute, China Academy of Railway Sciences Co., Ltd. and National Key Laboratory of High-Speed Railway Track System, China Academy of Railway Sciences Co., Ltd. The remaining authors declare that the research was conducted in the absence of any commercial or financial relationships that could be construed as a potential conflict of interest.

## Appendix A

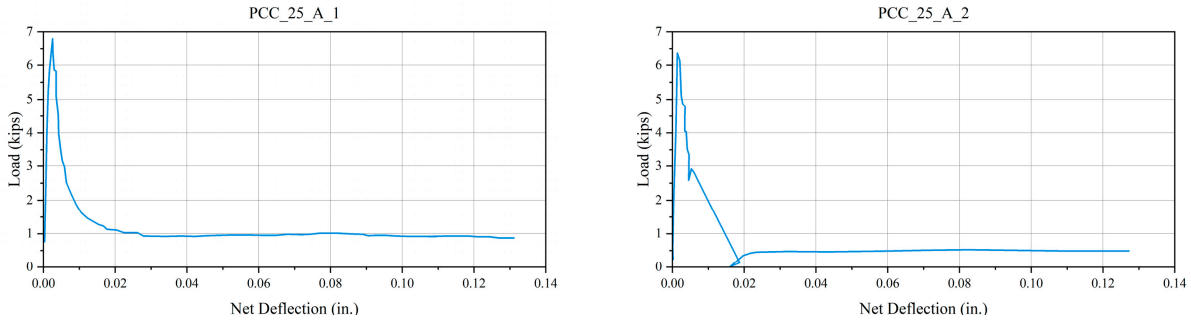



**Figure A1.** *Cont.*

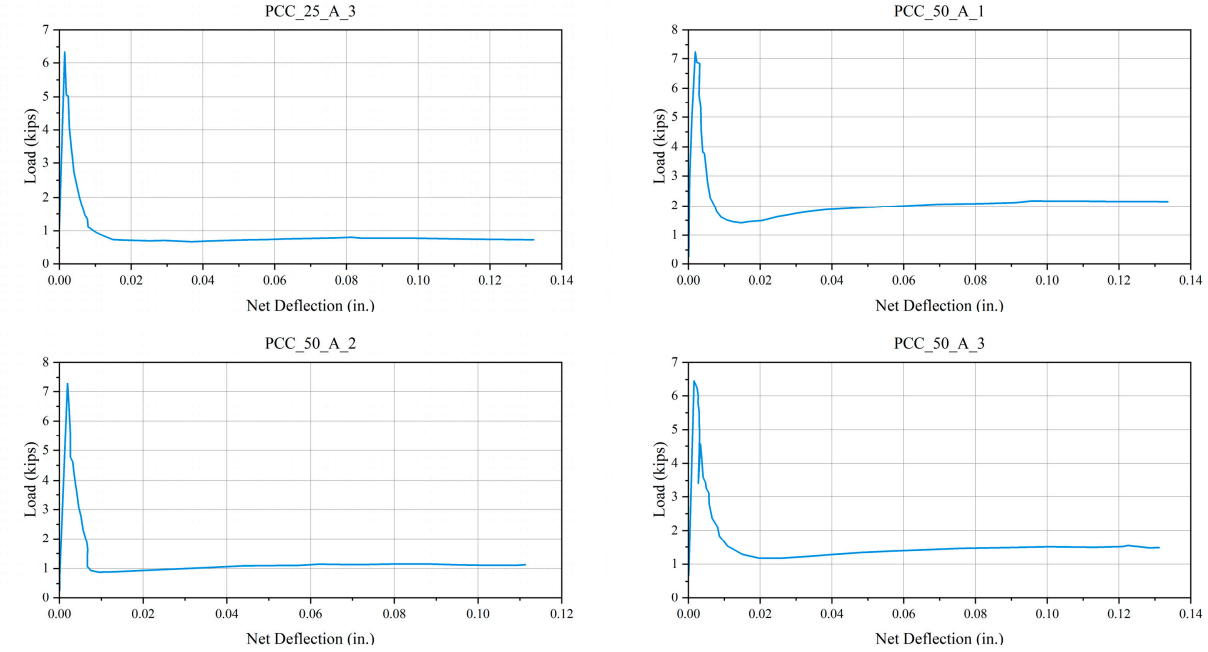



**Figure A1.** Load-deflection Curve and PCC with fiber A Curves.

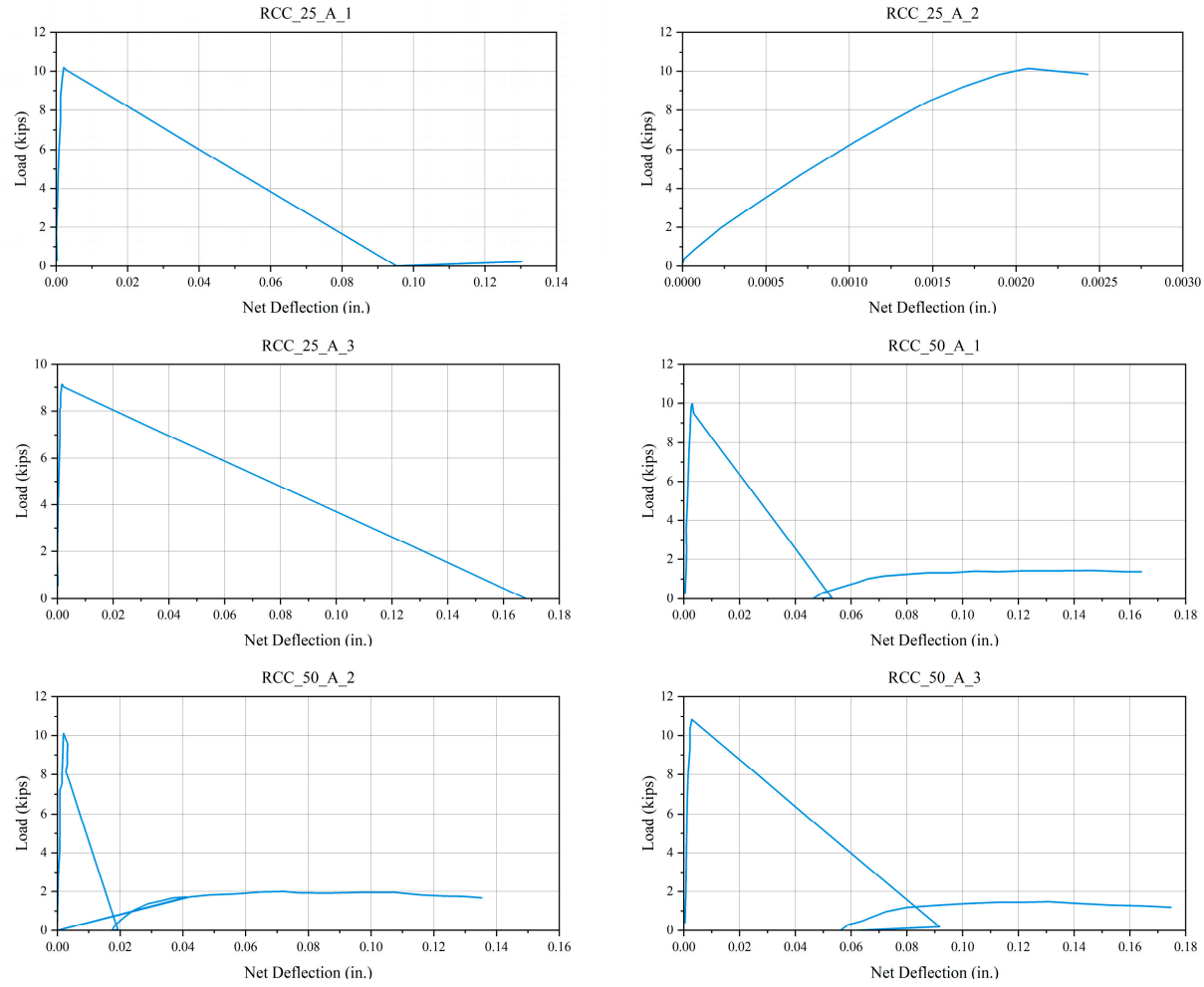



**Figure A2.** RCC with fiber A Curves.

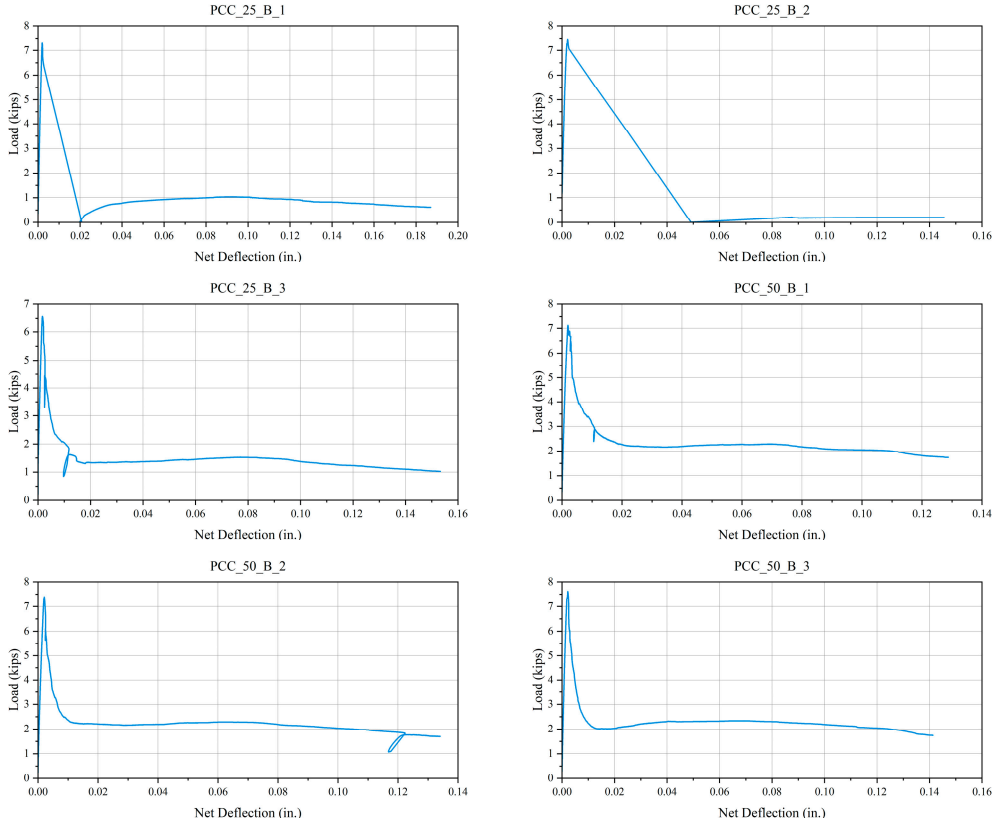



**Figure A3.** PCC with fiber B Curves.

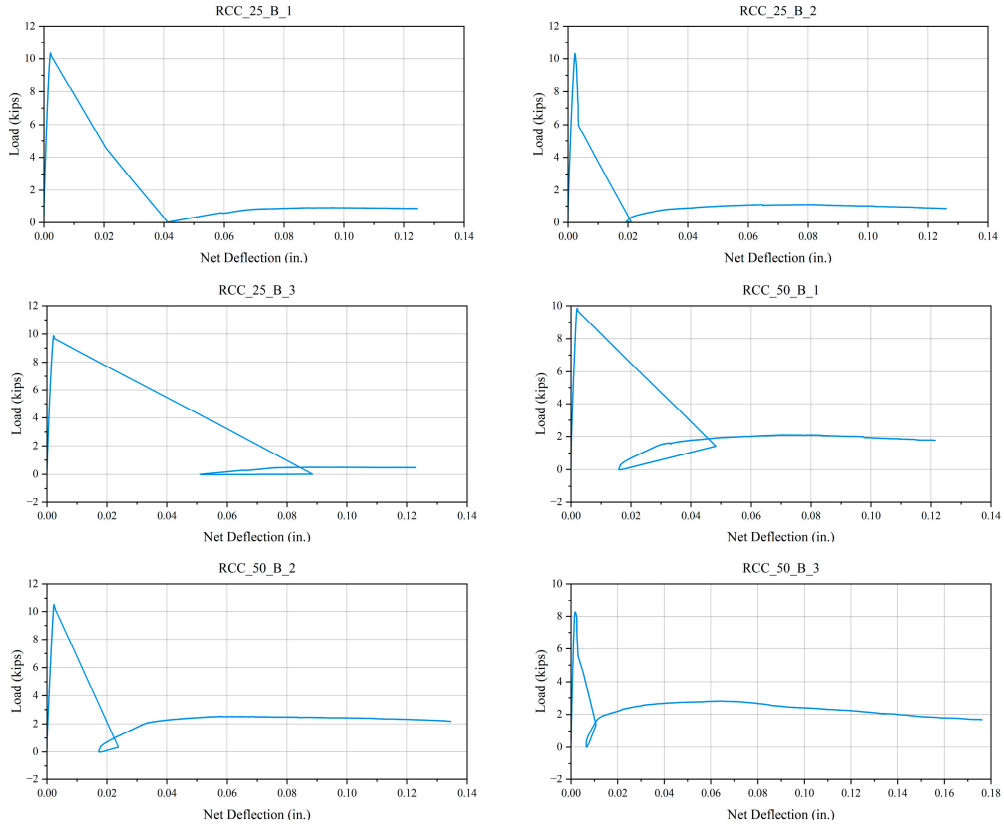



**Figure A4.** RCC with fiber B Curves.

## Appendix B

**Table A1.** Beam Specimens Dimensions after cracking.

| | Depth | | Width | | Ave. Depth | Ave. Width |
|---|---|---|---|---|---|---|
| RCCA25_3 | 6.261 | 6.093 | 6.176 | 6.205 | 6.18 | 6.19 |
| RCCA50_1 | 6.169 | 6.089 | 6.223 | 6.214 | 6.13 | 6.22 |
| RCCA25_1 | 6.064 | 6.039 | 6.117 | 6.198 | 6.05 | 6.16 |
| RCCA50_3 | 6.030 | 6.131 | 6.212 | 6.263 | 6.08 | 6.24 |
| RCCA50_2 | 6.262 | 6.043 | 6.200 | 6.120 | 6.15 | 6.16 |
| RCCA25_2 | 6.085 | 6.117 | 6.157 | 6.170 | 6.10 | 6.16 |
| PCCA50_3 | 6.077 | 6.042 | 6.071 | 6.104 | 6.06 | 6.09 |
| PCCA25_2 | 6.103 | 6.041 | 6.158 | 6.165 | 6.07 | 6.16 |
| PCCA25_3 | 6.104 | 6.057 | 6.165 | 6.224 | 6.08 | 6.20 |
| PCCA50_2 | 5.979 | 6.047 | 6.125 | 6.088 | 6.01 | 6.11 |
| PCCA25_1 | 6.094 | 6.019 | 6.124 | 6.131 | 6.06 | 6.13 |
| PCCA50_1 | 6.065 | 6.142 | 6.150 | 6.158 | 6.10 | 6.15 |
| RCCB50_3 | 6.072 | 6.323 | 6.19 | 6.18 | 6.20 | 6.19 |
| RCCB50_2 | 6.06 | 6.06 | 6.166 | 6.17 | 6.06 | 6.17 |
| RCCB50_1 | 6.083 | 6.223 | 6.29 | 6.164 | 6.15 | 6.23 |
| RCCB25_1 | 6.122 | 6.201 | 6.22 | 6.172 | 6.16 | 6.20 |
| RCCB25_3 | 6.28 | 6.078 | 6.202 | 6.203 | 6.18 | 6.20 |
| RCCB25_2 | 6.036 | 6.091 | 6.158 | 6.177 | 6.06 | 6.17 |
| PCCB50_1 | 6.047 | 5.955 | 6.147 | 6.146 | 6.00 | 6.15 |
| PCCB50_2 | 6.055 | 6.2 | 6.183 | 6.137 | 6.13 | 6.16 |
| PCCB25_1 | 6.052 | 6.062 | 6.18 | 6.17 | 6.06 | 6.18 |
| PCCB50_3 | 6.135 | 6.063 | 6.17 | 6.15 | 6.10 | 6.16 |
| PCCB25_3 | 6.054 | 6.044 | 6.082 | 6.084 | 6.05 | 6.08 |
| PCCB25_2 | 6.07 | 6.033 | 6.14 | 6.148 | 6.05 | 6.14 |

## Appendix C

**Table A2.** Testing result of ASTM C1609/C1609M.

| **MOR** | **[MPa]** | | | | | | | |
|---|---|---|---|---|---|---|---|---|
| Mixture ID | PCC A 0.25 | PCC A 0.5 | PCC B 0.25 | PCC B 0.5 | RCC A 0.25 | RCC A 0.5 | RCC B 0.25 | RCC B 0.5 |
| 1 | 4.160 | 4.379 | 4.462 | 4.229 | 6.240 | 5.864 | 6.070 | 5.764 |
| 2 | 3.848 | 4.580 | 4.577 | 4.410 | 6.077 | 5.975 | 6.270 | 6.400 |
| 3 | 3.819 | 4.003 | 4.070 | 4.585 | 5.363 | 6.493 | 5.753 | 4.798 |
| Average | 3.942 | 4.321 | 4.370 | 4.408 | 5.893 | 6.111 | 6.031 | 5.654 |
| variation | 0.036 | 0.086 | 0.071 | 0.032 | 0.217 | 0.113 | 0.068 | 0.651 |
| st.dev | 0.189 | 0.293 | 0.266 | 0.178 | 0.466 | 0.336 | 0.261 | 0.807 |
| COV | 4.795 | 6.776 | 6.082 | 4.039 | 7.910 | 5.501 | 4.327 | 14.267 |
| $F_{600}$ | [MPa] | | | | | | | |
| | PCC A 0.25 | PCC A 0.5 | PCC B 0.25 | PCC B 0.5 | RCC A 0.25 | RCC A 0.5 | RCC B 0.25 | RCC B 0.5 |
| 1 | 0.572 | 1.060 | 0.369 | 1.288 | | | | 0.886 |
| 2 | 0.273 | 0.636 | | 1.286 | | 0.835 | 0.433 | 1.068 |
| 3 | 0.446 | 0.751 | 0.832 | 1.328 | | | | 1.456 |
| Average | 0.430 | 0.816 | 0.601 | 1.301 | | 0.835 | 0.433 | 1.137 |
| variation | 0.023 | 0.048 | 0.107 | 0.001 | | | | 0.085 |
| st.dev | 0.150 | 0.219 | 0.327 | 0.024 | | | | 0.291 |

**Table A2.** *Cont.*

| **MOR** | **[MPa]** | | | | | | | |
|---|---|---|---|---|---|---|---|---|
| $F_{600}$ | [MPa] | | | | | | | |
| COV | 34.847 | 26.899 | 54.464 | 1.810 | | | | 25.622 |
| $F_{150}$ | [MPa] | | | | | | | |
| | PCC A 0.25 | PCC A 0.5 | PCC B 0.25 | PCC B 0.5 | RCC A 0.25 | RCC A 0.5 | RCC B 0.25 | RCC B 0.5 |
| 1 | 0.572 | 1.317 | 0.566 | 1.076 | | 0.831 | 0.502 | 1.042 |
| 2 | 0.294 | 0.590 | 0.122 | 1.208 | | 1.064 | 0.543 | 1.415 |
| 3 | 0.471 | 0.895 | 0.763 | 1.227 | | 0.870 | 0.277 | 1.295 |
| Average | 0.446 | 0.934 | 0.484 | 1.170 | | 0.921 | 0.441 | 1.251 |
| variation | 0.020 | 0.133 | 0.108 | 0.007 | | 0.016 | 0.020 | 0.036 |
| st.dev | 0.141 | 0.365 | 0.328 | 0.082 | | 0.125 | 0.143 | 0.190 |
| COV | 31.546 | 39.070 | 67.880 | 7.019 | | 13.542 | 32.455 | 15.207 |
| $T_{150}$ | [N-m] | | | | | | | |
| | PCC A 0.25 | PCC A 0.5 | PCC B 0.25 | PCC B 0.5 | RCC A 0.25 | RCC A 0.5 | RCC B 0.25 | RCC B 0.5 |
| 1 | 16.439 | 28.425 | | 31.983 | | | | |
| 2 | | | | 31.081 | | | | |
| 3 | 12.816 | 16.169 | 21.315 | 31.991 | | | | |
| Average | 14.627 | 22.297 | 21.315 | 31.685 | | | | |
| variation | 6.561 | 75.106 | | 0.274 | | | | |
| st.dev | 2.562 | 8.666 | | 0.523 | | | | |
| COV | 17.512 | 38.868 | | 1.651 | | | | |

## Appendix D



**Figure A5.** Beam Specimens RCC_A_0.25_1.



**Figure A6.** Beam Specimens RCC_A_0.25_2.



**Figure A7.** Beam Specimens RCC_A_0.25_3.



**Figure A8.** Beam Specimens RCC_A_0.5_1.



**Figure A9.** Beam Specimens RCC_A_0.5_2.



**Figure A10.** Beam Specimens RCC_A_0.5_3.

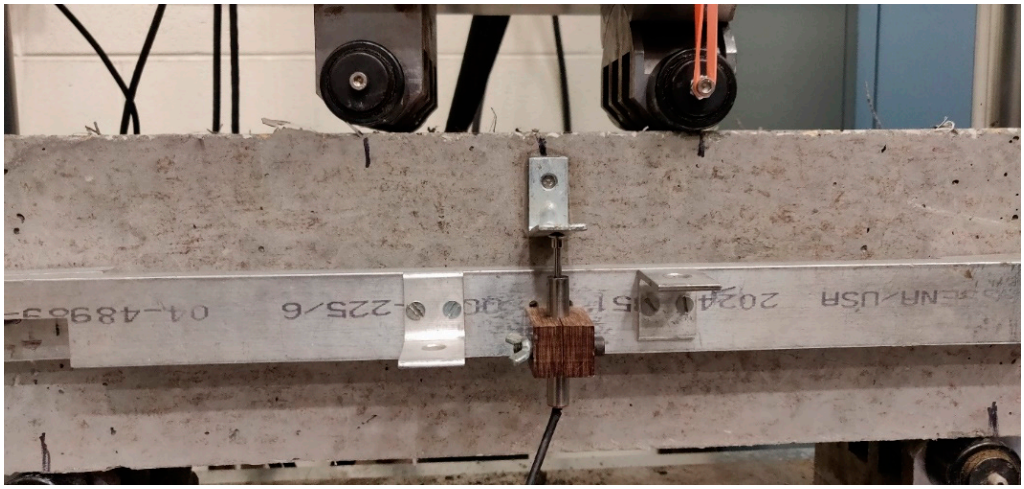


**Figure A11.** Beam Specimens RCC_B_0.5_1.



**Figure A12.** Beam Specimens RCC_B_0.5_2.



**Figure A13.** Beam Specimens RCC_B_0.5_3.



**Figure A14.** Beam Specimens PCC_A_0.25_1.



**Figure A15.** Beam Specimens PCC_A_0.25_2.



**Figure A16.** Beam Specimens PCC_A_0.25_3.



**Figure A17.** Beam Specimens PCC_A_0.5_1.



**Figure A18.** Beam Specimens PCC_A_0.5_2.



**Figure A19.** Beam Specimens PCC_A_0.5_3.

## Appendix E



**Figure A20.** Cylinder Specimens PCC_B_0.25_1.



**Figure A21.** Cylinder Specimens PCC_B_0.25_2.



**Figure A22.** Cylinder Specimens PCC_B_0.25_3.



**Figure A23.** Cylinder Specimens PCC_B_0.5_1.



**Figure A24.** Cylinder Specimens PCC_B_0.5_2.




**Figure A25.** Cylinder Specimens PCC_B_0.5_3.

## Appendix F




**Figure A26.** FiberA_BarChip MQ58.

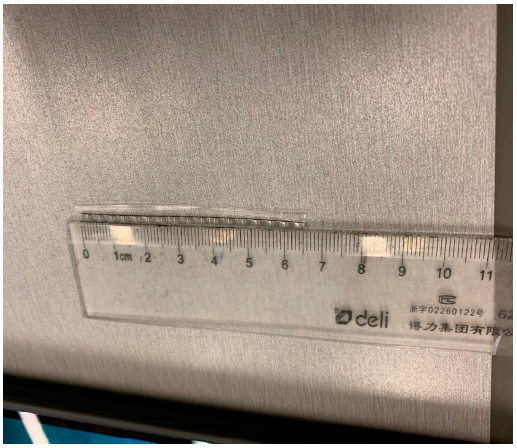



**Figure A27.** FiberB_Fibermesh 4 Roads.

## References


1. Piggott, R.W. *Roller-Compacted Concrete Pavements: A Study of Long Term Performance*; Portland Cement Association: Washington, DC, USA, 1999.
2. Portland Cement Association. *Structural Design of Roller-Compacted Concrete for Industrial Pavements*; Portland Cement Association: Washington, DC, USA, 1987.
3. Pittman, D.W. *Development of a Design Procedure for Roller-Compacted Concrete (RCC) Pavements*; The University of Texas at Austin: Austin, TX, USA, 1993.
4. LaHucik, J.R.; Roesler, J.R. Material Constituents and Proportioning for Roller-Compacted Concrete Mechanical Properties. FHWA-ICT-18-014. 2018. Available online: https://www.ideals.illinois.edu/items/106960/bitstreams/348834/data.pdf (accessed on 31 August 2018).
5. Harrington, D.; Abdo, F.; Ceylan, H.; Adaska, W.; Hazaree, C.; Bektas, F. Guide for Roller-Compacted Concrete Pavements. 2010. Available online: https://rccpavementcouncil.org/wp-content/uploads/2016/08/CP-Tech-Center-RCC-2010.pdf (accessed on 31 August 2018).
6. LaHucik, J.; Dahal, S.; Roesler, J.; Amirkhanian, A.N. Mechanical properties of roller-compacted concrete with macro-fibers. *Constr. Build. Mater.* **2017**, *135*, 440–446. [CrossRef]
7. Salimi, A.; Kamboozia, N.; Aliha MR, M. Experimental Investigation of the self-healing capability of Roller-Compacted Concrete (RCC) containing epoxy-filled glass tubes through fracture properties. *Case Stud. Constr. Mater.* **2024**, *21*, e03369. [CrossRef]
8. Achilleos, C.; Hadjimitsis, D.; Neocleous, K.; Pilakoutas, K.; Neophytou, P.O.; Kallis, S. Proportioning of steel fibre reinforced concrete mixes for pavement construction and their impact on environment and cost. *Sustainability* **2011**, *3*, 965–983. [CrossRef]
9. Altoubat, S.A.; Roesler, J.R.; Lange, D.A.; Rieder, K.A. Simplified method for concrete pavement design with discrete structural fibers. *Constr. Build. Mater.* **2008**, *22*, 384–393. [CrossRef]
10. Wang, Z.; Hu, H.; Papastergiou, P.; Angelakopoulos, H.; Guadagnini, M.; Pilakoutas, K. Effect of fibre length on the mechanical properties of SFRC using recycled Steel fibres. *Constr. Build. Mater.* **2024**, *415*, 134890. [CrossRef]
11. Otieno, M.; Mushunje, K. Creep deformation characteristics of rubberised structural concrete. *Constr. Build. Mater.* **2021**, *312*, 125418. [CrossRef]
12. Isa, M.N.; Pilakoutas, K.; Guadagnini, M.; Angelakopoulos, H. Mechanical performance of affordable and eco-efficient ultra-high performance concrete (UHPC) containing recycled tyre steel fibres. *Constr. Build. Mater.* **2020**, *255*, 119272. [CrossRef]
13. Akhtar, T.; Ali, B.; Kahla, N.B.; Kurda, R.; Rizwan, M.; Javed, M.M.; Raza, A. Experimental investigation of eco-friendly high strength fiber-reinforced concrete developed with combined incorporation of tyre-steel fiber and fly ash. *Constr. Build. Mater.* **2022**, *314*, 125626. [CrossRef]
14. Alwesabi, E.A.; Bakar, B.A.; Alshaikh, I.M.; Zeyad, A.M.; Altheeb, A.; Alghamdi, H. Experimental investigation on fracture characteristics of plain and rubberized concrete containing hybrid steel-polypropylene fiber. In *Structures*; Elsevier: Amsterdam, The Netherlands, 2021; Volume 33, pp. 4421–4432. [CrossRef]
15. Neves, A.; Almeida, J.A.; Miranda, T.; Cunha, V.M.; Pereira, E. Self-healing assessment and variability in plain and recycled tyre fiber reinforced concrete based on tensile splitting test. *J. Build. Eng.* **2024**, *84*, 108567. [CrossRef]
16. Yang, G.; Cheng, F.; Zuo, S.; Zhang, J.; Xu, Y.; Hu, Y.; Hu, X.; Wei, Y.; Gou, G. Constructing quasi-vertical fiber bridging behaviors of aramid pulp at interlayer of laminated basalt fiber reinforced polymer composites to improve flexural performances. *Chin. J. Aeronaut.* **2023**, *36*, 477–488. [CrossRef]
17. Meyyappan, P.L.; Carmichael, M.J. Studies on strength properties of basalt fibre reinforced concrete. *Mater. Today Proc.* **2021**, *43*, 2105–2108. [CrossRef]
18. Alomayri, T. Performance evaluation of basalt fiber-reinforced geopolymer composites with various contents of nano $CaCO_3$. *Ceram. Int.* **2021**, *47*, 29949–29959. [CrossRef]
19. Yildizel, S.A.; Tayeh, B.A.; Uzun, M. The evaluation of calcium carbonate added and basalt fiber reinforced roller compacted high performance concrete for pavement. *Case Studies in Constr. Mater.* **2022**, *17*, e01293. [CrossRef]
20. Wang, X.; Jin, Y.; Huang, W.; Li, X.; Ma, Q. Effect of hybrid basalt and sisal fibers on durability and mechanical properties of lightweight roadbed foam concrete. *Case Stud. Constr. Mater.* **2023**, *19*, e02592. [CrossRef]
21. Mitani, E.; Ozaki, Y.; Sato, H. Two types of CO· · · HO hydrogen bonds and OH· · · OH (dimer, trimer, oligomer) hydrogen bonds in PVA with 88% saponification/PMMA and PVA with 99% saponification/PMMA blends and their thermal behavior studied by infrared spectroscopy. *Polymer* **2022**, *246*, 124725. [CrossRef]
22. Yao, J.; Ge, Y.; Ruan, W.; Meng, J. Effects of PVA fiber on shrinkage deformation and mechanical properties of ultra-high performance concrete. *Constr. Build. Mater.* **2024**, *417*, 135399. [CrossRef]
23. Min, W.L.; Jin, W.L.; He, X.Y.; Wu, R.J.; Chen, K.Y.; Chen, J.J.; Xia, J. Experimental study on the flexural fatigue performance of slag/fly ash geopolymer concrete reinforced with modified basalt and PVA hybrid fibers. *J. Build. Eng.* **2024**, *94*, 109917. [CrossRef]
24. Rao, L.; Wang, L.; Zheng, Y. Experimental research on mechanical properties and compression constitutive relationship of PVA fiber-reinforced coral concrete. *Materials* **2022**, *15*, 1762. [CrossRef]
25. Wan, X.; Shen, C.; Wang, P.; Zhao, T.; Lu, Y. A study on fracture toughness of ultra-high toughness geopolymer composites based on Double-K Criterion. *Constr. Build. Mater.* **2020**, *251*, 118851. [CrossRef]

26. Gencel, O.; Bayraktar, O.Y.; Kaplan, G.; Arslan, O.; Nodehi, M.; Benli, A.; Gholampour, A.; Ozbakkaloglu, T. Lightweight foam concrete containing expanded perlite and glass sand: Physico-mechanical, durability, and insulation properties. *Constr. Build. Mater.* **2022**, *320*, 126187. [CrossRef]
27. Ibrahim KI, M. Recycled waste glass powder as a partial replacement of cement in concrete containing silica fume and fly ash. *Case Studies in Constr. Mater.* **2021**, *15*, e00630. [CrossRef]
28. Zeybek, Ö.; Özkılıç, Y.O.; Karalar, M.; Çelik, A.I.; Qaidi, S.; Ahmad, J.; Burduhos-Nergis, D.D.; Burduhos-Nergis, D.P. Influence of replacing cement with waste glass on mechanical properties of concrete. *Materials* **2022**, *15*, 7513. [CrossRef] [PubMed]
29. Ali, B.; Raza, S.S.; Hussain, I.; Iqbal, M. Influence of different fibers on mechanical and durability performance of concrete with silica fume. *Struct. Concr.* **2021**, *22*, 318–333. [CrossRef]
30. Gholampour, A.; Danish, A.; Ozbakkaloglu, T.; Yeon, J.H.; Gencel, O. Mechanical and durability properties of natural fiber-reinforced geopolymers containing lead smelter slag and waste glass sand. *Constr. Build. Mater.* **2022**, *352*, 129043. [CrossRef]
31. Jamshaid, H.; Mishra, R.K.; Raza, A.; Hussain, U.; Rahman, M.L.; Nazari, S.; Chandan, V.; Muller, M.; Choteborsky, R. Natural cellulosic fiber reinforced concrete: Influence of fiber type and loading percentage on mechanical and water absorption performance. *Materials* **2022**, *15*, 874. [CrossRef]
32. Sreekumaran, S.; Krishna, A.; Karuppanan, K. Opening and out-of-plane shear fracture performance of steel and natural sisal hybrid fiber reinforced concrete. *Struct. Concr.* **2024**. [CrossRef]
33. Fischer Kerche, E.; Silveira Caldas, B.G.; Carvalho, R.F.; Amico, S.C. Mechanical response of sisal/glass fabrics reinforced polyester–polyethylene terephthalate foam core sandwich panels. *J. Sandw. Struct. Mater.* **2022**, *24*, 1993–2009. [CrossRef]
34. *C192/C192M-18*; Making and Curing Concrete Test Specimens in the Laboratory. ASTM International: West Conshohocken, PA, USA, 2018.
35. *ASTM C39/C39M-12*; Standard Test Method for Compressive Strength of Cylindrical Concrete Specimens. ASTM International: West Conshohocken, PA, USA, 2012.
36. *C1609/C1609M-12*; Standard Test Method for Flexural Performance of Fiber-Reinforced Concrete (Using Beam with Third-Point Loading). ASTM International: West Conshohocken, PA, USA, 2010.
37. *C1435/C1435M-14*; Standard Practice for Molding Roller-Compacted Concrete in Cylinder Molds Using a Vibrating Hammer. ASTM International: West Conshohocken, PA, USA, 2014.
38. *D1557-12*; Standard Test Methods for Laboratory Compaction Characteristics of Soil Using Modified Effort (56,000 ft-lbf/ft3 (2700 kN-m/$m^3$)). ASTM International: West Conshohocken, PA, USA, 2012.
39. Banthia, N.; Islam, S.T. Loading rate concerns in ASTM C1609. *J. Test. Eval.* **2013**, *41*, 1032–1036. [CrossRef]
40. Amirkhanian, A.; Roesler, J. *Overview of Fiber-Reinforced Concrete Bridge Decks*; Iowa Department of Transportation: Ames, IA, USA, 2019.
41. Li, S.; Zhou, Z.; Lu, Y.; Wang, Z.; An, J. Effects of polyvinyl alcohol fiber content on early crack resistance and shrinkage properties of high ductility geopolymer concrete. *J. Dalian Univ. Technol./Dalian Ligong Daxue Xuebao* **2024**, *64*, 74–81. [CrossRef]


**Disclaimer/Publisher's Note:** The statements, opinions and data contained in all publications are solely those of the individual author(s) and contributor(s) and not of MDPI and/or the editor(s). MDPI and/or the editor(s) disclaim responsibility for any injury to people or property resulting from any ideas, methods, instructions or products referred to in the content.